Investigation of in-situ lithium dendrite growth in the garnet type electrolyte

Li<sub>7-x</sub>La<sub>3</sub>Zr<sub>2-x</sub>Ta<sub>x</sub>O<sub>12</sub> (LLZTO) under an applied DC voltage

Chong Lei, Michael F. Simpson\* and Anil V. Virkar

Department of Materials Science and Engineering

University of Utah

122 S. Central Campus Drive

Salt Lake City, UT 84112

\*Corresponding author (michael.simpson@utah.edu)

Keywords: solid state electrolyte, batteries, lithium, dendrites, LLZTO

## Abstract

A translucent Al-containing garnet type electrolyte (Al-LLZTO) with high lithium-ion conductivity was made by pressure filtration followed by sintering to study in-situ lithium dendrite growth. A transparent tube furnace was built for in-situ dendrite growth studies above room temperature. In-situ lithium dendrite growth in a garnet-type electrolyte under an applied DC voltage was investigated at three different temperatures (room temperature, 100°C, and 200°C (above the melting point of lithium)). Critical current density (CCD) was estimated based on a previous model developed for sodium dendrites (which are actually filaments) in Na-β"-alumina. The CCD defined here is different than most of the reported work in lithium and lithium-ion batteries. When the temperature is higher than room temperature but lower than the melting point of lithium, lithium dendrites grow rapidly. However, when the temperature is above the melting point of lithium, no lithium dendrites were observed under similar testing conditions. This is because the CCD for liquid lithium dendrites to form is much higher than that for solid lithium

dendrites to form. Approximate estimates of the CCD below and above the melting point of lithium are also given. This investigation provides significant insights into dendrite (filament) growth above room temperature, and possible prevention of lithium dendrites in working solid-state lithium-ion batteries, and the efficiency improvement of solid-state batteries.

## Introduction

With the increasing demand for energy storage, the next generation of energy storage/conversion devices need to be developed [1–3]. Adoption of fully electric vehicles (EVs) is rapidly increasing. It has been predicted that EVs could make-up half of new car sales by 2025 and the majority of the inventory of private vehicles by 2030 [4]. EVs require reliable and efficient energy storage/conversion devices with high energy density and power density [5,6]. The graphite anode currently used in lithium-ion batteries (LIBs) has relatively low Li storage capacity based on formation of LiC<sub>6</sub> at the anode (8.8 wt% Li, 372 mAh/g). Recently, it has been reported that graphene layers could be used to go to higher Li loading. Specifically, it might be possible to form LiC or Li<sub>2</sub>C<sub>2</sub> compounds with greater than 1000 mAh/g capacity [7]. Replacement of the graphite anode with a pure lithium metal anode would increase the energy storage density to 3862 mAh/g (100 wt% Li) [8]. However, direct contact of the reactive lithium metal with organic liquid electrolytes can cause safety problems since many of the organic liquid electrolytes are flammable and toxic. Battery failure in a traditional battery with flammable liquid electrolytes can contribute to dangerous fires. Because of safety concerns, all-solid-state batteries are of interest since flammable organic electrolytes can be avoided [9,10]. In all-solid-state batteries, ceramic oxides are used as electrolytes for fast transport of metal ions. With solid-state electrolytes, safety and durability of batteries can be significantly improved [11,12]. Also, batteries with ceramic electrolytes can be operated over a wider temperature range.

The fundamental requirements for the solid electrolyte are high metal ion conductivity, negligible electronic conductivity, high mechanical strength, good interfacial compatibility, and long cycle life with minimal degradation. Recently, a Ta-doped garnet type lithium-ion conductor, Li<sub>7-x</sub>La<sub>3</sub>Zr<sub>2-x</sub>Ta<sub>x</sub>O<sub>12</sub> (LLZTO), exhibiting good electrochemical performance with high lithiumion conductivity (>10<sup>-4</sup> Scm<sup>-1</sup> at room temperature), was developed [13,14]. However, even in allsolid-state batteries, electrolyte degradation and the formation of metallic dendrites (filaments) can lead to battery failure. Recently, Alexander et al. [15] have demonstrated excellent performance and stability of lithium batteries using porous mixed ionic conductor (MIEC)/LLZ electrolyte/MIEC porous electrode with very stable performance and high current density. Most of the work still has been with traditional approach, without porous MIEC electrodes. Typically, dendrites of near circular cross section form in batteries made of liquid electrolytes. In solid electrolytes, the geometry is more of a filament or a ribbon type. This is because from the standpoint of elastic strain energy developed in the solid electrolyte, the filament or ribbon type geometry is favored. This is because, for a circular cross-section of the dendrite, strain energy in the solid is much higher than with filament (with thin elliptical cross-section) as the geometry. However, since much of the literature uses the word 'dendrite', this usage is made here also. But, it is to be noted that they are actually filaments or ribbons. Recently, Wang et al. [16] have investigated the mechanism and the kinetics of lithium dendrite growth in liquid electrolytes. It is important to investigate the mechanism of lithium dendrite growth in solid electrolytes, including how it varies with temperature. Since the transparency of typical solid-state electrolyte is usually low, our group [17] has developed a translucent Al-containing garnet electrolyte (Al-LLZTO) by pressure filtration followed by sintering to investigate lithium dendrite growth. Pressure-filtration allows the attainment of a high green density, which subsequently leads to higher sintered density, and translucent samples. The electrolyte has comparable density and lithium-ion conductivity to the electrolyte (slightly higher) made by dry processing and sintering.

Many researchers have examined lithium dendrite growth in solid electrolytes [8,18,19]. Wang et al. [20] reported that lithium dendrite growth rate in garnet exhibits a linear relationship with the current density under an applied DC voltage. The dendrites prefer to grow at cracks, open pores, and grain boundaries in LLZTO electrolyte when the current density is above some critical value [20–22]. Ren et al. [23] confirmed that lithium dendrites in short-circuited garnet electrolyte grow through grain boundaries and interconnected pores using SEM after applying direct current for a duration of time at room temperature. They observed that after dendrites go through the electrolyte, the cell resistance drops to near zero. They demonstrated this by also conducting electrochemical impedance spectroscopy. They also ethanol-leached the cells after dendrite formation. Lithium was leached into ethanol. This confirms that formed dendrites are of lithium. At the present time, solid-state batteries with solid electrolytes exhibit lower power density than LIBs with organic liquid electrolytes mainly because of poor interfacial contact between the electrodes and the solid electrolyte [24,25]. However, increasing the temperature leads to higher lithium ion conductivity [17,26,27]. It may be desirable to operate cells with lithium ion conducting solid electrolytes above the melting point of lithium metal (~180.5°C) [28,29]. This has also been shown by Kinzer et al. [30]. When the battery is operated above the melting point of lithium, the liquid lithium will be in direct contact with the solid electrolyte. The mechanism of lithium dendrite growth in a solid electrolyte when lithium metal is liquid could be different from that when lithium metal is solid.

Mainly, critical current density for growth is expected to be much higher due to low viscosity of molten lithium.

Typically, two types of experiments have been conducted for studying lithium dendrite growth; (1) disk-type sample sandwiched between two lithium foils under an applied DC voltage (or under a fixed current; galvanostatic) [23], (2) disk-type sample sandwiched between two lithium foils subjected to typically a square cycling of current (changing between positive and negative current) and measuring the corresponding voltage cycles. In the former, lithium transports only in one direction. Typically, the corresponding voltage slowly increases (indicating some degradation of lithium/solid electrolyte interfaces) with an abrupt drop in voltage to near zero indicating lithium dendrite has shorted the electrolyte. Experiments are often conducted under a current density of ~0.5 mA/cm<sup>2</sup> or sometimes even smaller [23]. In the cycling experiments, the magnitude of the voltage typically increases in a given cycle, and also it keeps increasing with increasing cycles, indicating that the polarization resistance increases [31]. Eventually, the voltage drops to near zero, indicating that a dendrite (or dendrites) has (have) gone through the electrolyte and shorted the cell. In many studies, the current density at which shorting occurs is defined as the critical current density (CCD). Figure 1 shows schematics of the typically observed results in the two different types of tests. An important point is that in the former type of test, it has been observed that degradation and failure occur at current densities as low as 0.01 mA/cm<sup>2</sup> indicating that CCD must be even lower than this value.

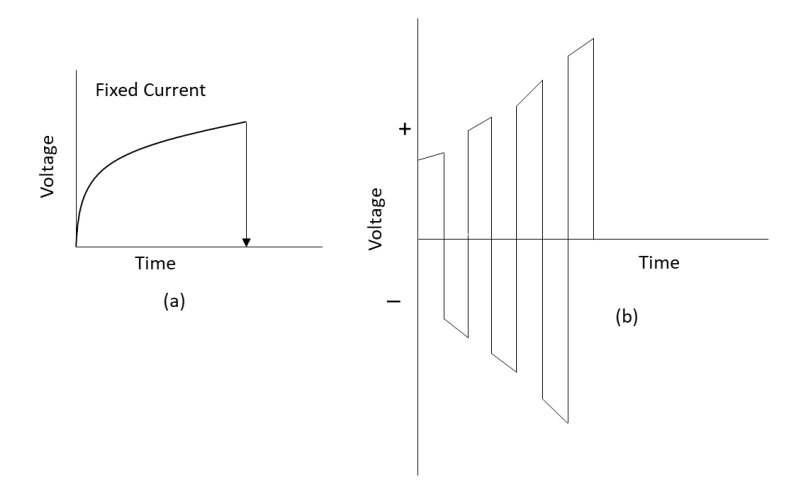


Figure: 1(a) Typical DC polarization test (galvanostatic). Abrupt drop in voltage indicates shorting of the cell due to dendrites. (b) Typical cycling test in which direction of the current is alternated. Magnitude of the voltage typically increases and eventually drops to zero indicating shorting of the cell due to dendrites.

During the 1960's through the 1980's, extensive work was conducted on high temperature (~300°C) sodium sulfur batteries in which both electrodes are liquid and Na-β"-alumina is the solid electrolyte [32-34]. Typical charging current densities were on the order of 250 mA/cm². Under certain conditions, dendrites formed through the electrolyte and sometimes caused fires. Several models were developed for the determination of the critical current density (CCD) [35-37]. The CCD in those models were under galvanostatic conditions. The models were based on mechanical properties (fracture toughness or critical stress intensity factor or fracture surface energy), crack (or dendrite or filament) geometry, dimensions, and viscosity of liquid sodium. Typical values of the CCD experimentally measured were on the order of several A/cm². Early models were based on two-dimensional fracture mechanics, which grossly overestimated the CCD (several hundred A/cm²) [37]. Subsequently, Virkar and Viswanathan solved (approximately) the three-dimensional model for dendrite growth and demonstrated that the CCD is on the order of a

few A/cm² in accordance with experimental work [38]. The models were based on the pressure exerted on the crack (dendrite or more correctly filament) surface by the flowing liquid sodium. Thus, the dendrite dimensions were naturally included, and the CCD was found to be inversely proportional to viscosity of liquid sodium. Virkar and Viswanathan [39] in another work also demonstrated that if the temperature of the experiment is lowered below the melting temperature of sodium, dendrites immediately formed even at a few mA/cm² current densities consistent with vast increase in 'viscosity' (pseudo-viscosity) when the formed sodium is solid. In lithium batteries operated at room temperature or below the melting point of lithium (which is ~180°C), lithium dendrites are expected to form at even lower current densities, as observed in much of the reported literature. Also, yield stress of lithium is higher than that of solid sodium, thus the expected CCD is even lower. Indeed, recent work on Na-ion batteries shows that higher current densities can be passed through the electrolyte compared to lithium-based batteries [40].

Viswanathan and Virkar [41] investigated sodium dendrite growth in Na-β"-alumina experimentally and theoretically. They subjected bar-shaped samples to electrolysis with one side painted with silver paint and the other submerged in NaNO3 solution in water. A current density of 5 mA/cm² was passed for a period of time (up to a maximum of 30 s). After electrolysis, samples were fractured in four-point bending tests. Crack (dendrite) length was estimated using the Griffith equation. Samples were electrolyzed over a range of temperatures from 0 to 60°C. They observed that the crack velocity increased with increasing temperature. Crack velocity was found to be several microns per second. The crack velocity exhibited Arrhenius equation with activation energy close to that of sodium ion conduction in Na-β"-alumina.

In the present work, study of dendrite growth was conducted under DC conditions, so that lithium (as ions) flow in only one direction; there is no cycling. The present work thus differs from much of the reported work. Also, the objective of the work was to examine dendrite formation in which one or a few dendrites are formed. This is also different from many studies in which a solid electrolyte disk is sandwiched between two lithium foils. In such cases, many dendrites can form through the electrolyte disk. Also, in the present work, by virtue of the geometry of the test, the ohmic resistance is much larger than the polarization resistance. As a result, as dendrite grows, the ohmic resistance decreases. This leads to a decrease in voltage (as the distance between the tip of the dendrite and the other lithium electrode decreases). By contrast, in most studies on disks with foil electrodes placed on the circular sides of the disks, often in a galvanostatic experiment, voltage initially increases because of the degradation of the electrodes and interfaces.

For the experiments reported here, a transparent tube furnace was built to investigate lithium dendrite growth in a translucent LLZTO electrolyte above room temperature (100°C) and 200°C (above the melting point of lithium)). Lithium dendrite growth at room temperature was investigated by using an optical microscope. Lithium dendrite growth was studied at each temperature mentioned above.

## **Experimental**

Figure 2 shows the process used for making translucent Al-LLZTO disks by pressure filtration followed by sintering [17]. Al-containing Li<sub>6.75</sub>La<sub>3</sub>Zr<sub>1.75</sub>Ta<sub>0.25</sub>O<sub>12</sub> (Al-LLZTO) powder was first made by a solid-state method. Stoichiometric amounts of LiOH·H<sub>2</sub>O, (Sigma-Aldrich, 99.0%), La<sub>2</sub>O<sub>3</sub> (Alfa Aesar, 99.99%, calcined at 900°C for 12 h before using), ZrO<sub>2</sub> (Sigma-Aldrich,

99.0%), Ta<sub>2</sub>O<sub>5</sub> (Sigma-Aldrich, 99.99%), and Al<sub>2</sub>O<sub>3</sub> (Alfa Aesar, 99.9% - 0.15 mol per mol LLZTO) were mixed in 2-propanol by planetary milling for 8 h. Excess of 15wt% LiOH was added to compensate for lithium loss during pressure filtration and during sintering. Then the powder was calcined at 900°C for 6 h after drying. The as-calcined powder was mixed again in 2-propanol and planetary milled for 13 h. The mixed powder was ground by mortar and pestle after drying to break down the soft agglomerates. 70wt% Al-LLZTO water suspension was made, and 0.1 mg m<sup>-2</sup> of dispersant (DARVAN C-N, Vanderbilt Minerals LLC, Norwalk, CT) was added to the suspension to minimize flocculation. The suspension was ultrasonicated before pressure filtration to further break down the soft agglomerates. The ultrasonicated Al-LLZTO suspension was then used for pressure filtration. The disks made by pressure filtration were dried at 100°C for 48 h in air. The disks were then buried in the calcined powder to minimize lithium loss during sintering. The disks were sintered at 1180°C in air for 4 h.

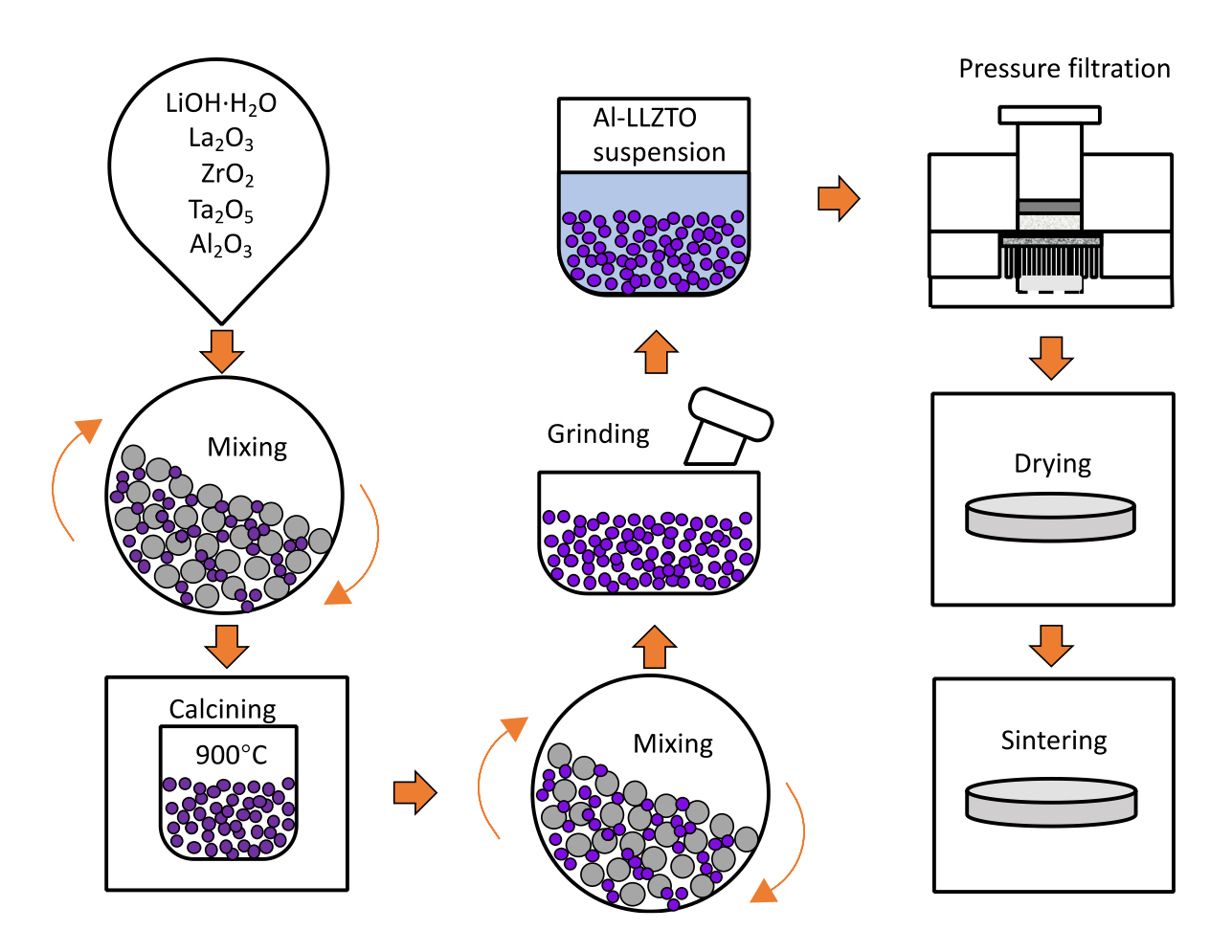


Figure 2. Fabrication process for making translucent Al-LLZTO disks.

The sintered disks were used for the investigation of lithium dendrite growth. A transparent tube furnace was built by using a quartz tube (outside diameter: 50 mm) illustrated in Figure 3(a). Two pieces of heating tape (Omega HTWAT Series, silicone rubber, 2ft) were wrapped around the quartz tube from the ends, respectively. A transparent window was left open in the middle of the quartz tube so that light could go through the Al-LLZTO disk, and lithium dendrite growth could be captured by a digital camera (Sony ZV-1) from the top. Fiberglass wool with an outer layer of aluminum foil was used to isolate the tube furnace to minimize heat loss. The furnace can go up to ~230°C, which is well above the melting point of lithium metal. A schematic of the electrochemical cell is shown in Figure 3(b). Two pieces of lithium chips (surface area: ~0.5 cm²,

thickness: 0.6 mm) were placed at each end on the same surface of the Al-LLZTO disk. The distance between the two lithium chips was ~0.8 cm. No pressure was applied to the chips to control the contact area with the disk. The lithium chips were connected to a voltage generator (BK precision DC regulated power supply 1621 A), and two Keithley 6514 meters (one for current measurement, and the other for voltage measurement) by using the current collectors that protruded out of the furnace. The temperature of the transparent tube furnace was measured by a K-type thermocouple and a multimeter. The whole testing setup was placed into the tube furnace for the investigation of lithium dendrite growth above room temperature. A similar testing setup was used for the investigation of dendrite growth at room temperature, and a 10 k $\Omega$  resistor was used at room temperature to protect the Keithley 6514 meters. Also, instead of using lithium chips directly as electrodes, a silver wire (polarized as the anode) and a silver wire (polarized as the cathode) were used to accurately locate the lithium dendrite initial point. Instead of using the transparent tube furnace, an optical microscope in transmission mode (AmScope ME520T) was used to observe the dendrites. All tests were done in an argon-filled glove box (Mbraun Labstar Pro) with <10 ppm  $O_2$  and  $H_2O$ .

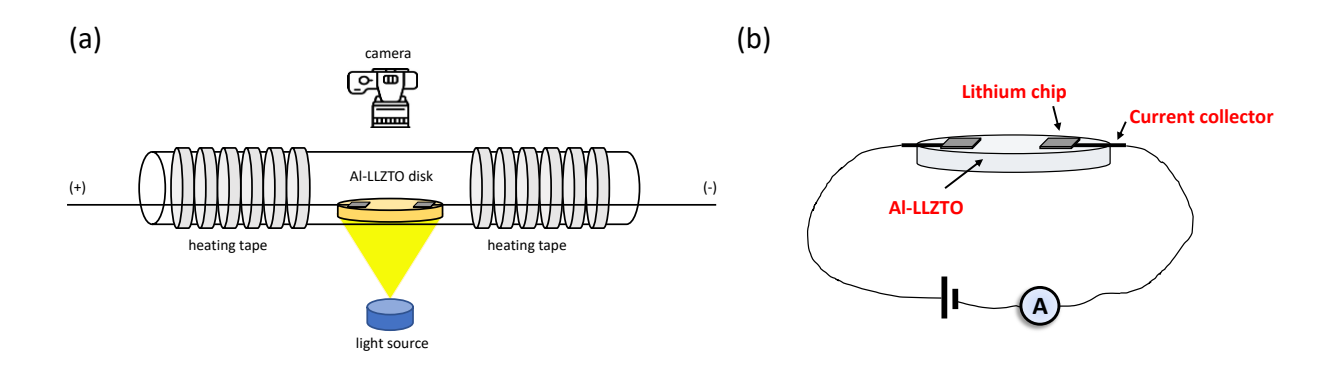


Figure 3. A schematic of (a) the transparent tube furnace and (b) the testing setup.

## **Results**

First, lithium dendrite growth was investigated at room temperature using an optical microscope. The two lithium chips were polarized as cathode and anode. At the anode, the reaction  $Li \rightleftharpoons Li^+ + e^-$  occurs, where lithium is oxidized to lithium ions. At the cathode, the reaction  $Li^+ + e^- \rightleftharpoons Li$  occurs, where lithium ions are reduced to lithium, and lithium dendrites grow from the cathode. Electrons flow through the external circuit. Only a small voltage needs to be applied to initiate the dendrites, since the reaction is  $Li \rightarrow Li$ . Figure 4 shows the current passing through the Al-LLZTO disk (black) and the voltage measured across the current collectors (red) as functions of time during the experiment performed at room temperature. The voltage across the current collectors decreases, and the current passing through the Al-LLZTO disk increases, which likely indicates the formation and growth of lithium dendrites. The jaggedness of the curves is due to the fact that dendrites do not grow in a straight line and also that bifurcation of the dendrites occurs. The original voltage applied across the two current collectors was 3 V, and it decreased to about 0.9 V after 300 s. The current increased from about 0.06 to 0.25 mA.

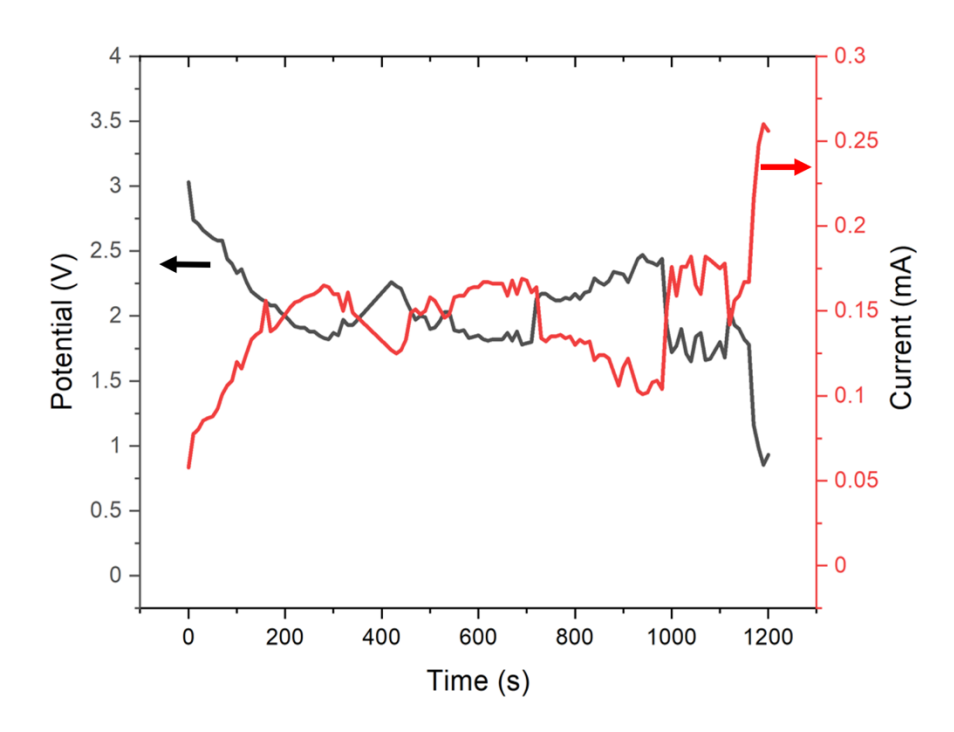


Figure 4. Current passing through the Al-LLZTO disk (red) and voltage measured across the current collectors (black) at room temperature.

Figure 5 shows photos captured under an optical microscope that indicate lithium dendrite growth occurred from 0 to 300 s. After 300 s, the experiment was stopped. By using the microscope, a specific small region of the lithium dendrites can be clearly observed. During dendrite growth, some dendrites bifurcated, and some went out of view. The jaggedness of the current-voltage curves is due to nonlinear and bifurcated dendrites.

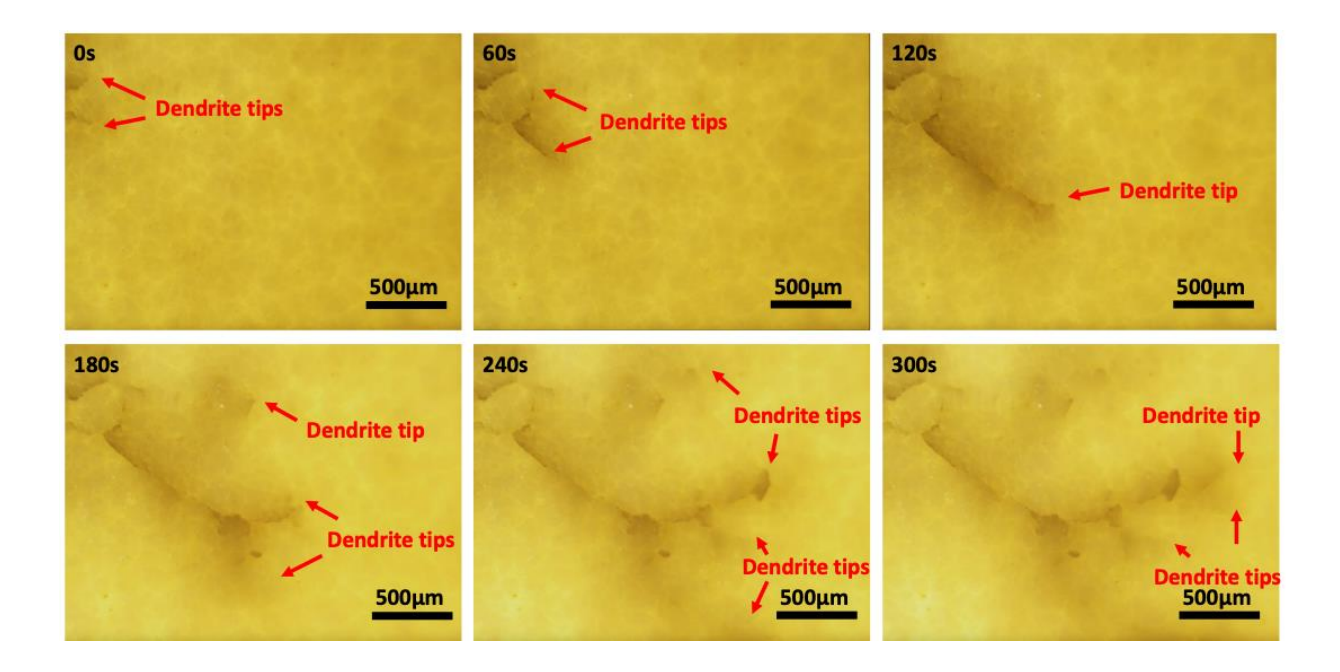


Figure 5. Digital photos of the Al-LLZTO sample taken under the optical microscope during dendrite formation and growth from 0 to 300 s at room temperature.

Figure 6 shows a digital photo of lithium dendrites formed in the Al-LLZTO disk at room temperature after the completion of the experiment. The lithium dendrites exhibit a tree-shaped outline.



Figure 6. A digital photo of the Al-LLZTO disk after lithium dendrite formation and growth at room temperature.

The lithium dendrites formed and grew even when the current was as small as 0.06 mA at room temperature. The net charge (in coulombs) was calculated to be 0.17 C by integrating the current over time. This corresponds to about 12.2 µg of lithium dendrites formed.

An important difference between many reported results in the literature either under a DC voltage or cycling (Figure 1) on discs with lithium electrodes covering the two surfaces of the disk is that multiple dendrites occur penetrating the disc. In the present study, typically only one dendrite forms but can bifurcate as seen in Figures 5 and 6. To be clear, this was not due to any intentional control. Also, in most reported tests conducted on disks (under galvanostatic conditions) with electrodes applied on the disk surfaces, voltage increases until a sudden drop occurs due to dendrites shorting (Figure 1), which suggests that the polarization resistance keeps increasing. In fact, many have attributed this to interface degradation. In the present work, the dominant resistance is the ohmic resistance between the dendrite tip and the other electrode. Thus, as dendrites become longer, the ohmic resistance decreases. This allows one to actually be able to investigate growth of the dendrites and also observe the bifurcation of dendrites, which is difficult to investigate when electrodes are applied on the two opposite surfaces of a disk sample.

The transparent tube furnace was used for investigating lithium dendrite growth above room temperature. The first temperature used for testing was 100°C, which is above room temperature

but below the melting point of lithium. Figure 7 shows the current passing through the Al-LLZTO disk (red) and the voltage measured across the current collectors (black) as a function of time at 100°C. The applied voltage across the current collectors was held stable at 3V from 30 to 180 s. The current passing through the Al-LLZTO disk increased with the progression of time, reaching 2.1 mA after 180 s. Figure 8 shows digital photos of Al-LLZTO during dendrite formation and growth from 0 to 180 s at 100°C. There were no dendrites, and only a clear translucent Al-LLZTO disk was observed before the voltage was applied across the current collectors. After the voltage was applied for 60 s, a lithium dendrite formed at the cathode lithium chip. As the voltage difference was maintained, more and more lithium dendrites formed in the Al-LLZTO disk. Note that under a fixed applied voltage at 3V, the current keeps increasing, in accordance with expectations that dendrites are getting longer and the distance that ions must transport through the electrolyte decreases. The experiment was stopped before the lithium dendrites could short out the Al-LLZTO disk. By integrating the current over time, the net charge passed during dendrite growth was calculated to be 0.27 C, which corresponds to about 19.4 µg of lithium dendrites formed. This dendrite growth experiment was performed only for 180 s, which is much shorter than the similar experiment conducted at room temperature (1200 s), but more lithium dendrites formed. This is likely because the lithium ion conductivity of Al-LLZTO is higher at 100°C than that at room temperature. The ionic conductivities of the Al-LLZTO made by pressure filtration and sintering are 1.47×10<sup>-4</sup> and 2.26×10<sup>-3</sup> Scm<sup>-1</sup> at 23 and 100°C, respectively [17]. Higher lithium ion conductivity may facilitate faster lithium dendrite growth. Indeed, Viswanathan and Virkar [41] measured dendrite growth in Na-β"-alumina and observed an increase in crack growth rate with an increase in temperature, attributed to higher sodium ion conductivity of the electrolyte at higher temperatures. In another lithium dendrite growth experiment at 100°C, the resistance between the two electrodes was measured every 60 s (the current was stopped, and the resistance was measured by a Keithley 2000 meter). The measured resistance was 2.7, 2.3, 1.8, 1.2 k $\Omega$  at 0, 60, 120, 180 s, respectively. The decreasing resistance is consistent with formation of lithium dendrites. Also, the measured resistance was approximately the same as the resistance calculated by the measured voltage and current from the other experiment (see Figure 7) using Ohm's law. This is because the ohmic resistance of the electrolyte is much higher than the polarization resistance of the electrodes, and the effective width of the electrolyte (for the purposes of resistance calculations) decreases as dendrites grow. Note that CCD for solid state Li metal batteries has been reported to increase with increasing temperature [42], which seems to contradict the increased rate of dendrite growth from room temperature to 100°C. This can be ascribed to competing temperature effects (lithium viscosity, ionic conductivity, interfacial conductivity). Ultimately more experiments of this nature are needed at more temperature values to understand lithium dendrite behavior in LLZTO.

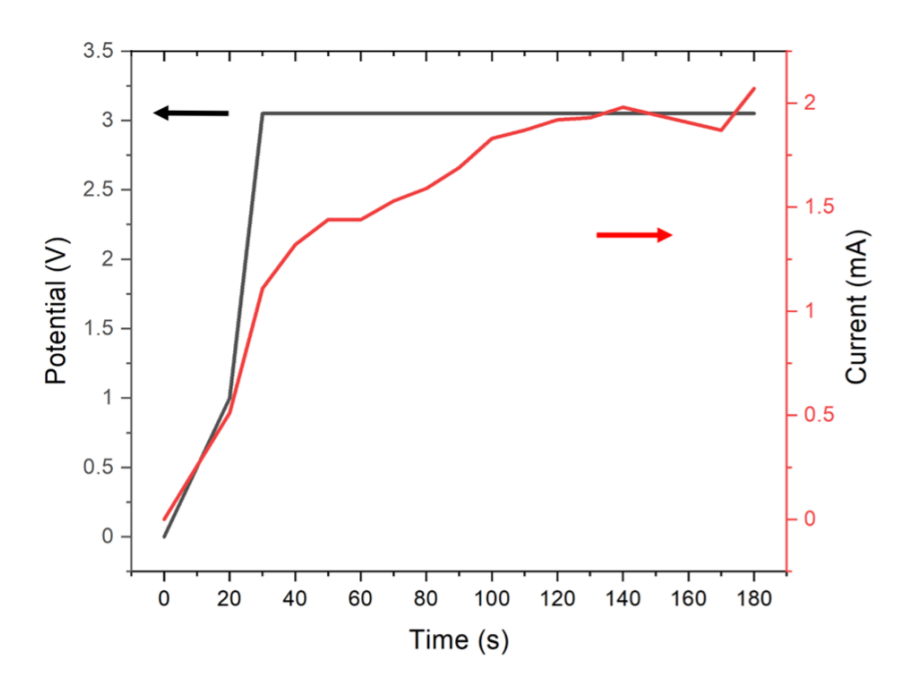


Figure 7. Current passing through the Al-LLZTO disk (red), and voltage measured across the current collectors (black) during lithium dendrite growth at 100°C.

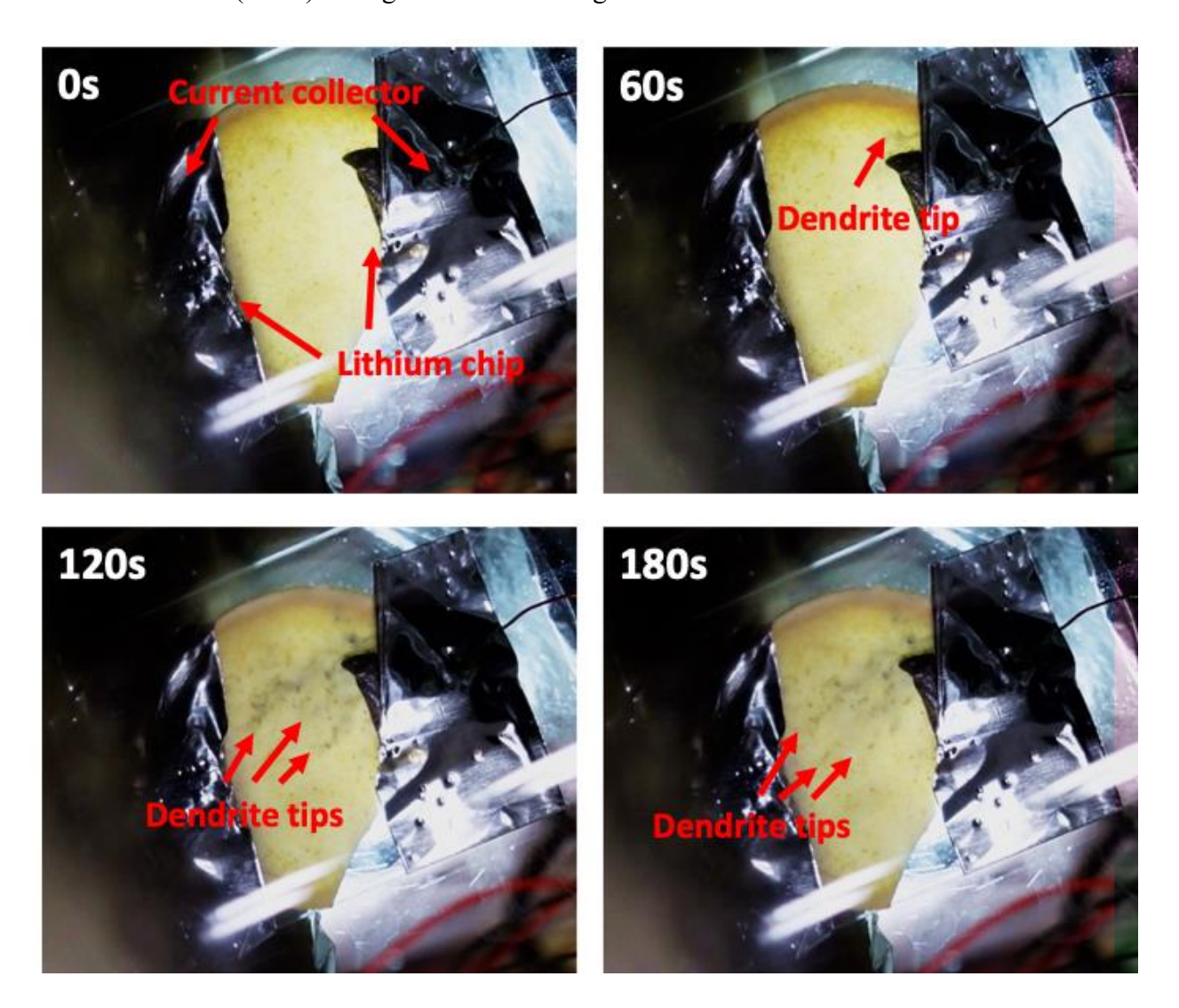


Figure 8. Digital photos of the Al-LLZTO during dendrite formation and growth from 0 to 180 s at  $100^{\circ}$ C.

Figures 9 and 10 show the results of a dendrite growth experiment conducted at ~200°C, which is above the melting point of lithium. The current passing through the Al-LLZTO disk (black) and the voltage measured across the current collectors (red) are shown in Figure 9. The applied voltage was progressively increased to see if the current could reach a value at which liquid lithium

dendrite would form. The current passing through Al-LLZTO increased with an increasing voltage across the current collectors. However, no dendrites formed even after the voltage was applied for 780 s (Figure 10) and even when the current reached 17 mA. The electrolyte resistance also did not change throughout the experiment, as evidenced by the proportionality between potential and current shown in Figure 9. Note that in this run, there could have been some degree of dissolution of silver from the current collector to either lithium chip. This was not apparent from observation but cannot be disregarded without further analysis.

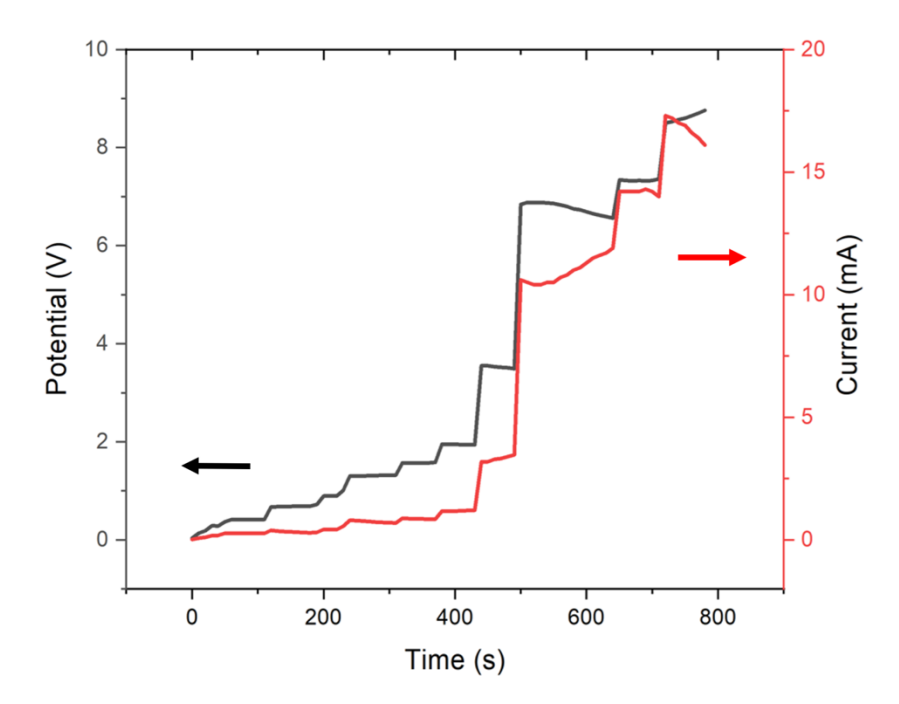


Figure 9. Current passing through the Al-LLZTO disk (red) and voltage measured across the current collectors (black) during lithium dendrite growth at ~200°C, which is above the melting point of lithium.

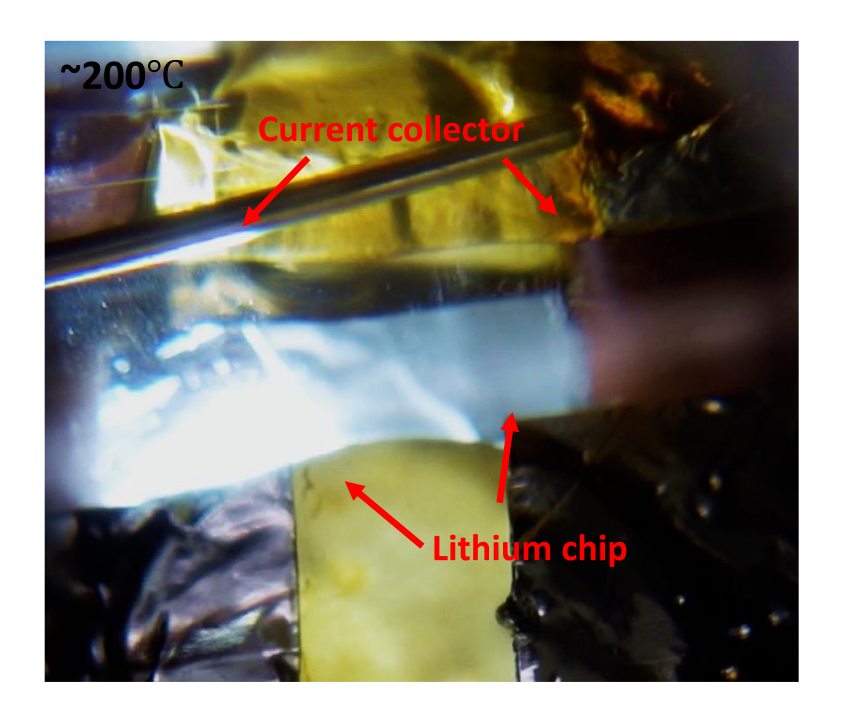


Figure 10. Digital photo of the Al-LLZTO after voltage applied for 780 s at ~200°C. No dendrites formed.

## **Discussion**

In many solid electrolytes, dendrites or cracks can form electrochemically. In reference [43], Virkar has addressed the issue of crack/dendrite nucleation. It has been shown that if the applied voltage across suitably placed electrodes exceeds a certain critical value, dendrites/cracks can initiate at atomic level defects. The equation is given by

$$E_A \ge E_{cr} = E_o \left\{ \sqrt{\frac{\pi}{(1 - v^2)c}} \frac{K_{lc}}{2p_o} \right\}$$

where  $E_o$  is a constant,  $K_{Ic}$  is the fracture toughness of the material,  $\nu$  is Poisson's ratio, c is crack radius and  $p_o$  is the atmospheric pressure. For most materials the value of the critical voltage is a fraction of a volt. For example, Lim and Virkar [44] showed that in zirconia-based bi-layer samples (one layer is zirconia with 5% ceria added) ~0.2 V corresponds to ~715 atm of pressure. Under

this condition, an internal crack forms and grows. Most of the reported work has been on measuring/calculating the growth of dendrites. When considering growth, relevant parameter is the critical current density for the growth of an existing crack/dendrite, which depends on dendrite geometry including its length. The corresponding applied voltage, again across suitably placed electrodes, thus need be even lower. Nature of interfaces has been thus of great interest in many battery studies, initially starting with sodium-sulfur batteries in the late 1970's and in 1980's.

Extensive research has been conducted on Na-β"-alumina electrolyte used in Na-S batteries in the 1970's and 1980's, as previously mentioned. Na-S batteries typically operate at 300°C, well above the melting point of Na (~99°C). Charging current densities are usually ~250 mAcm<sup>-2</sup>. Only under certain conditions, such as nonwetted areas in contact with liquid sodium, do dendrites form. The present observations that no dendrites were observed at currents as high as 17 mA are consistent with observations made in Na-S batteries, although it is difficult to know what the exact current densities were in the present work due to the complicated geometry. In Na-S batteries, typically tubes of ~3 cm diameter with a wall thickness ~2 mm are used, and the geometry is well-defined. Nevertheless, the present results can be examined in light of results in Na-S batteries and theoretical models developed for dendrite growth in sodium ion conductors.

Virkar and Viswanathan [38] examined the growth of sodium dendrites in sodium ion conductors. That project investigated the growth of sodium dendrites during charging. In the earlier models which investigated two-dimensional crack models, the Hagen-Poiseuille equation was used; it was assumed that sodium formed at the tip of a crack and flowed into the liquid sodium anode [35-37]. When the current density exceeded some critical value, crack extension occurred; which depended

on fracture mechanical properties of Na- $\beta$ "-alumina, crack length and the viscosity of liquid sodium. The pressure distribution on the crack surface was nearly linearly dependent on distance along the crack, with the highest being at the tip. The calculated values of the critical current density were orders of magnitude higher than actually observed. This was attributed to the fact that the actual geometry is like a filament, and not a two-dimensional crack. Virkar and Viswanathan [38] later examined the problem of sodium filament with length l and width l (Figure 11). The cross-section was assumed to be elliptical, with the minor diameter, l determined by the local sodium pressure, using linear elasticity [38]. It was shown that the pressure along the length of the filament, l (l), is given by equation (2)

$$P(y) = \left(\frac{2\eta V_m E^3}{(1 - v^2)F}\right)^{\frac{1}{4}} \left(\frac{il^2}{c^4}\right)^{\frac{1}{4}} y^{\frac{1}{4}}$$
 (2)

where  $\eta$  is the viscosity of liquid sodium,  $V_m$  is the molar volume of liquid sodium, i is the current density, l is the length of the dendrite (filament), 2c is the width of the dendrite, v is the Poisson's ratio of the electrolyte, E is the Young's modulus of the electrolyte, F is the Faraday constant, and y is distance along the length of the dendrite measured from the surface of the electrolyte. An important point to note is that even though the Hagen-Poiseuille law was used, the pressure as a function of y is not linear in y, because the minor diameter of the elliptical shaped cross-section of the dendrite is position-dependent; the smallest at the electrolyte surface (electrolyte/electrode interface) and the largest near the tip of the dendrite. When P(l) reaches a critical value,  $P_{cr}$ , is given by equation 3.

$$P_{cr} = \left(\frac{\pi E \gamma_{eff}}{2c(1 - \nu^2)}\right)^{\frac{1}{2}} \tag{3}$$

where  $\gamma_{eff}$  is the fracture surface energy, dendrite extension occurs. Dendrite extension occurs in a stable manner because it is dependent on the current density. That is, the load is created internally (by electrolysis) and thus catastrophic growth cannot occur [43]. From these equations, the CCD can be estimated, given by equation 3.

$$i_{cr} = \left(\frac{\pi (1 - \nu^2) F \gamma_{eff}^2}{8 V_m E \eta}\right) \left(\frac{c^2}{l^3}\right) \tag{4}$$

Note, this CCD is for the growth of a dendrite under an applied DC voltage. The calculated values of the critical current densities were in good agreement with experimental work [38]. Recently, Schmidt and Sakamoto [45] and Sarkar and Thangdurai [46] have qualitatively verified the above equation for the critical current density (CCD) for the growth of lithium dendrites.

In earlier work, Virkar and Viswanathan [39] conducted an experiment in which one end of a bar-shaped sample of Na-β"-alumina was painted with silver and the other end dipped in a solution of NaNO3 in water in which a silver wire was inserted. A small heater was placed near the silver-painted side, and the end was heated to ~120°C, which is above the melting point of sodium. Electrolysis was conducted such that sodium formed at the silver painted side. The current was several mA. No dendrites were observed. Slowly the temperature was lowered by turning down the power to the heater. As soon as the temperature was below the melting point of sodium, dendrites were observed. This was rationalized as due to a large increase in 'viscosity' when

sodium formed is solid. While viscosity is a property used to describe the flow of liquids, its use in certain soft solids is deemed reasonable. For example, a Bingham solid (which can exhibit elastic-plastic behavior when the applied stress exceeds yield stress) can be described as having viscosity [47].

The viscosity of liquid lithium at 200°C is  $\sim 6 \times 10^{-4} \text{ Nsm}^{-2}$ . Sharafi et al. [48] have measured fracture toughness of LLZO by using the indentation technique over a range of grain sizes. The values approximately 0.6 MPam<sup>1/2</sup> for large grain sizes. At 200°C, the expected CCD will be on the order several hundred mAcm<sup>-2</sup> to a few Acm<sup>-2</sup>. Thus, under the experimental conditions in this study, dendrites are not expected. Figure 11(a) shows a schematic of a possible dendrite. In such a case, the formed liquid lithium is expected to come out of the electrolyte without propagating (or forming) a dendrite. The yield stress of solid lithium at room temperature is  $\sim 7.5 \times 10^5 \text{ Nm}^{-2}$ . Assuming a shear rate of 0.1 s<sup>-1</sup>, the pseudo-viscosity will be  $\sim 7.5 \times 10^6 \text{ Nsm}^{-2}$ . Recently, Kinzer et al. [30] have also determined the relationship between pseudo-viscosity of solids and its relationship to critical current density for dendrite growth. Thus, the expected critical current density above which dendrites form is expected to be much lower than when the formed lithium is liquid; probably on the orders of nAcm<sup>-2</sup>. The total lithium being formed per unit time is given by

$$\dot{V} = \frac{i\pi l^2 V_m}{F} \tag{5}$$

which would be much greater than what can flow out of the electrolyte thus causing dendrite growth. Figure 11(b) shows a schematic. In this case, a dendrite will form (probably from a pre-

existing defect) and propagate into the electrolyte, as observed. For a given current density, when temperature is below the melting point of lithium, the rate of formation of lithium given by equation (5) remains the same. But since the viscosity is very high, the formed lithium cannot flow out. Thus, the only way it can be accommodated is by forming (extending) the dendrite or filament into the electrolyte – this is what one observes in a typical experiment. Thus, the rate of flow of liquid lithium in Figure 11(a) is nearly the same as the rate of dendrite extension in Figure 11(b). This rate is shown by a small extension at the tip of the filament in the electrolyte. But some lithium must flow out of the channel (dendrite, however small). One would thus expect there will be some uplift on the surface, which could be observed under a microscope if one can carefully remove the silver paint. Alternatively, one could use a layer of transparent conducting film (e.g. Indium Tin Oxide, ITO) in place of silver. This should allow one to observe part of the protruded lithium dendrite.

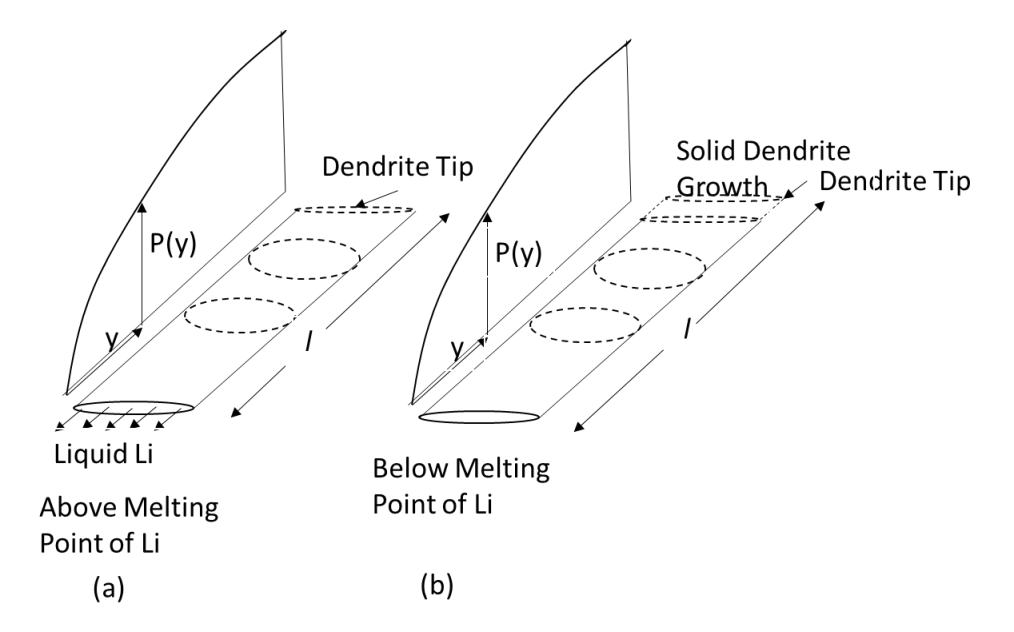


Figure 11. Possible liquid dendrite. (a) Liquid lithium formed will come out of the dendrite at a rate given by equation (4). (b) A solid dendrite will form and propagate into the electrolyte nearly at rate given by equation (4).

The observation in the present work, and the work of Kinzer et al. [30], that no dendrites were formed (over the range of experimental conditions used) when the temperature was above the melting point of lithium thus can be similarly explained. This observation also has some very important practical implications. One could design a lithium battery capable of operating just above the melting point of lithium. This could be achieved without substantially changing the battery design. For instance, one could envision using a metallic sponge at the anode. If the liquid lithium fully wets the metal, it will be retained in the metal sponge without causing any leakage. It may also be possible to use some solid metal that forms a solid alloy with lithium at the operating temperature of 200°C. A lithium battery operating just above the melting point of lithium would be able to deliver a high energy density as well as high power density. The use of sodium-sulfur battery was demonstrated for automotive applications during the 1980's. Lithium battery with a lower operating temperature (~200°C) and higher energy and power density could be a viable candidate for automotive applications. Such a lithium battery may also be useful for stationary energy storage.

## **Conclusions**

Al-LLZTO disks were made by pressure filtration followed by sintering. Lithium dendrite growth was investigated in Al-LLZTO disks over a range of temperatures from room temperature to 200°C, which is above the melting point of lithium. A quartz tube furnace was built to investigate lithium dendrite growth above room temperature. At temperatures below the melting point of lithium, lithium dendrites readily formed. No dendrites formed when the experiment was conducted at 200°C under similar testing conditions. The observation that dendrites readily formed

at room temperature but not at 200°C was attributed to much lower (pseudo) viscosity of lithium when it is liquid. Pseudo-viscosity of solid lithium, which can be estimated from its yield stress and shear rate by treating it as a Bingham solid [46], is orders of magnitude higher. Thus, dendrites readily form since lithium formed cannot easily flow out of the electrolyte. In terms of a fracture mechanical-electrochemical model developed previously [38], the critical current density at which dendrites form is much higher above the melting point of lithium than when it is solid. The present work shows that it may be possible to develop durable, high power density, and high energy batteries with lithium metal anode operating above the melting point of lithium.

# Acknowledgments

This work was supported in part by the National Science Foundation under grant number NSF-DMR-1742696 and in part Department of Energy Office of Basic Sciences under grant number DE-FG02-06ER46086.

#### References

- [1] J.B. Goodenough, Y. Kim, Challenges for rechargeable Li batteries, Chem. Mater. 22 (2010) 587–603. https://doi.org/10.1021/cm901452z.
- [2] H. Liu, X.B. Cheng, J.Q. Huang, H. Yuan, Y. Lu, C. Yan, G.L. Zhu, R. Xu, C.Z. Zhao, L.P. Hou, C. He, S. Kaskel, Q. Zhang, Controlling Dendrite Growth in Solid-State Electrolytes, ACS Energy Lett. 5 (2020) 833–843. https://doi.org/10.1021/acsenergylett.9b02660.
- [3] S.K. Heiskanen, J. Kim, B.L. Lucht, Generation and Evolution of the Solid Electrolyte Interphase of Lithium-Ion Batteries, Joule. 3 (2019) 2322–2333. https://doi.org/10.1016/j.joule.2019.08.018.
- [4] Y. Shi, F. Donghan, S. Yu, F. Chen, H. Li and Y. Zhou, "The projection of electric vehicle population considering scrapage and technology competetion: A case study in Shanghai",

- JUournal of Cleaner Production, 365 (2022) 132673.
- [5] J. Deng, C. Bae, J. Marcicki, A. Masias, T. Miller, Safety modelling and testing of lithiumion batteries in electrified vehicles, Nat. Energy. 3 (2018) 261–266. https://doi.org/10.1038/s41560-018-0122-3.
- [6] J.B. Goodenough, M.H. Braga, Batteries for electric road vehicles, Dalt. Trans. 47 (2018) 645–648. https://doi.org/10.1039/c7dt03026f.
- [7] Y. Yamada, J. Wang, S. Ko, E. Watnabe and A. Yamada, "Advances and issues in developing salt-concentrated battery electrolytes", Nature Energy, 4 No. 4 (2019) 269-280
- [8] F. Aguesse, W. Manalastas, L. Buannic, J.M.L. Del Amo, G. Singh, A. Llordés, J. Kilner, Investigating the dendritic growth during full cell cycling of garnet electrolyte in direct contact with Li metal, ACS Appl. Mater. Interfaces. 9 (2017) 3808–3816. https://doi.org/10.1021/acsami.6b13925.
- [9] F. Zheng, M. Kotobuki, S. Song, M.O. Lai, L. Lu, Review on solid electrolytes for all-solid-state lithium-ion batteries, J. Power Sources. 389 (2018) 198–213. https://doi.org/10.1016/j.jpowsour.2018.04.022.
- [10] J. Schnell, T. Günther, T. Knoche, C. Vieider, L. Köhler, A. Just, M. Keller, S. Passerini, G. Reinhart, All-solid-state lithium-ion and lithium metal batteries paving the way to large-scale production, J. Power Sources. 382 (2018) 160–175. https://doi.org/10.1016/j.jpowsour.2018.02.062.
- [11] T. Famprikis, P. Canepa, J.A. Dawson, M.S. Islam, C. Masquelier, Fundamentals of inorganic solid-state electrolytes for batteries, Nat. Mater. 18 (2019) 1278–1291. https://doi.org/10.1038/s41563-019-0431-3.
- [12] A. Manthiram, X. Yu, S. Wang, Lithium battery chemistries enabled by solid-state electrolytes, Nat. Rev. Mater. 2 (2017) 16103. https://doi.org/10.1038/natrevmats.2016.103.
- [13] Y. Wang, W. Lai, High ionic conductivity lithium garnet oxides of Li 7-xLa 3Zr 2-xTa xO 12 compositions, Electrochem. Solid-State Lett. 15 (2012) 3–7. https://doi.org/10.1149/2.024205esl.
- [14] M. Huang, T. Liu, Y. Deng, H. Geng, Y. Shen, Y. Lin, C.W. Nan, Effect of sintering

- temperature on structure and ionic conductivity of Li 7 XLa 3Zr 2O 12 0.5x (x =  $0.5 \sim 0.7$ ) ceramics, Solid State Ionics. 204–205 (2011) 41–45. https://doi.org/10.1016/j.ssi.2011.10.003.
- [15] G. V. Alexander, C. Shi, J O'Neil, E. D. Wachsman, 'Extreme lithium metal cycling enabled by mixed ion-and electron-conducting garnet three-dimensional architecture', Natrue Materials, 22 1136-1143 (2023).
- [16] Y. Wang, A. V. Virkar and X-D. Zhou, 'On the thermodynamic origin of the formation of Lidendrites in an electrochemical cell', J. Electrochem. Soc., (2021), 168, 100503.
- [17] C. Lei, D.K. Shetty, M.F. Simpson, A. V. Virkar, Fabrication of high-density and translucent Al-containing garnet, Li7–xLa3Zr2–xTaxO12 (LLZTO) solid-state electrolyte by pressure filtration and sintering, Solid State Ionics. 364 (2021) 115640. https://doi.org/10.1016/j.ssi.2021.115640.
- [18] W. Manalastas, J. Rikarte, R.J. Chater, R. Brugge, A. Aguadero, L. Buannic, A. Llordés, F. Aguesse, J. Kilner, Mechanical failure of garnet electrolytes during Li electrodeposition observed by in-operando microscopy, J. Power Sources. 412 (2019) 287–293. https://doi.org/10.1016/j.jpowsour.2018.11.041.
- Q. Li, T. Yi, X. Wang, H. Pan, B. Quan, T. Liang, X. Guo, X. Yu, H. Wang, X. Huang, L. Chen,
  H. Li, In-situ visualization of lithium plating in all-solid-state lithium-metal battery, Nano
  Energy. 63 (2019) 103895. https://doi.org/10.1016/j.nanoen.2019.103895.
- [20] D. Wang, K. Peng, Y. Fu, C. Zhu, Y. Yang, Kinetics of lithium dendrite growth in garnet-type solid electrolyte, J. Power Sources. 487 (2021) 229421. https://doi.org/10.1016/j.jpowsour.2020.229421.
- [21] E.J. Cheng, A. Sharafi, J. Sakamoto, Intergranular Li metal propagation through polycrystalline Li6.25Al0.25La3Zr2O12 ceramic electrolyte, Electrochim. Acta. 223 (2017) 85–91. https://doi.org/10.1016/j.electacta.2016.12.018.
- [22] T. Krauskopf, R. Dippel, H. Hartmann, K. Peppler, B. Mogwitz, F.H. Richter, W.G. Zeier, J. Janek, Lithium-Metal Growth Kinetics on LLZO Garnet-Type Solid Electrolytes, Joule. 3 (2019) 2030–2049. https://doi.org/10.1016/j.joule.2019.06.013.
- [23] Y. Ren, Y. Shen, Y. Lin, C.W. Nan, Direct observation of lithium dendrites inside garnet-

- type lithium-ion solid electrolyte, Electrochem. Commun. 57 (2015) 27–30. https://doi.org/10.1016/j.elecom.2015.05.001.
- [24] Q. Liu, Z. Geng, C. Han, Y. Fu, S. Li, Y. bing He, F. Kang, B. Li, Challenges and perspectives of garnet solid electrolytes for all solid-state lithium batteries, J. Power Sources. 389 (2018) 120–134. https://doi.org/10.1016/j.jpowsour.2018.04.019.
- [25] A. Ulvestad, A Brief Review of Current Lithium Ion Battery Technology and Potential Solid State Battery Technologies, ArXiv. (2018).
- [26] H. Xu, Y. Li, A. Zhou, N. Wu, S. Xin, Z. Li, J.B. Goodenough, Li3N-Modified Garnet Electrolyte for All-Solid-State Lithium Metal Batteries Operated at 40 °c, Nano Lett. 18 (2018) 7414–7418. https://doi.org/10.1021/acs.nanolett.8b03902.
- [27] J. Chen, J. Wu, X. Wang, A. Zhou, Z. Yang, Research progress and application prospect of solid-state electrolytes in commercial lithium-ion power batteries, Energy Storage Mater. 35 (2021) 70–87. https://doi.org/10.1016/j.ensm.2020.11.017.
- [28] J. Lang, K. Liu, Y. Jin, Y. Long, L. Qi, H. Wu, Y. Cui, A molten battery consisting of Li metal anode, AlCl3-LiCl cathode and solid electrolyte, Energy Storage Mater. 24 (2020) 412–416. https://doi.org/10.1016/j.ensm.2019.07.027.
- [29] Y. Jin, K. Liu, J. Lang, D. Zhuo, Z. Huang, C. an Wang, H. Wu, Y. Cui, An intermediate temperature garnet-type solid electrolyte-based molten lithium battery for grid energy storage, Nat. Energy. 3 (2018) 732–738. https://doi.org/10.1038/s41560-018-0198-9.
- [30] B. Kinzer, A. L. Davis, T. Krauskopf, H. Hartmann, W. S. LePage, E. Kazyak, J. Janek, N. P. Dasgupta and J. Sakamoto, 'Operando analysis of the molten Li/LLZO interface: Understanding how the physical properties of Li affect the critical current density', Matter 4, 1947-1961, June (2021).
- [31] X. Ke, Y. Wang, L. Dai and C. Yuan, "Cell failures of all solid state lithium metal batteries with inorganic electrolytes: Lithium dendrites", Energy Storage Materials, 33 (2020) 309-
- [32] J. Kummer and N. Weber, "A sodium-sulfur battery", Sae Transactions, (1968) 1003-1028.
- [33] S. P. Mitoff, M. W. Breiter and D. Chatterji, "Recent progress in development of sodiumsulfur battery for utility applicaion", 12<sup>th</sup> Intersociety Energy Conversion Engineering Conference, vol. 1, pp359-367 1977

- [34] W. Fischer, "state of development and prospects of sodium/sulfur batteries", Solid State lonics 3 (1981) 413-424.
- [35] R. H. Richman and G. J. Tennenhouse, "A model for degradation of ceramic electrolytes in Na-S batteries", J. A. Ceram. Soc. 58 [1-2] (1975) 63-67.
- [36] R. D. Armstrong, T. Dickinson and J. Turner, Electrochimica Acta, 19 (1974) 187--92
- [37] D. K. Shetty, A. V. Virkar and R. S. Gordon, pp 651-55 in Fracture Mechanics of ceramics, Vol. 4, edited by R. C. Bradt, D. P. H. Hasselman and F. F. Lange, Plenum New York, 1977.
- [38] A. V. Virkar, L. Viswanathan, A three-dimensional approach to the electrolytic degradation of solid electrolytes, J. Mater. Sci. 18 (1983) 1202–1212. https://doi.org/10.1007/BF00551990.
- [39] A. V. Virkar and L. Viswanathan, Sodium penetration in rapid ion conductors, J. Am. Ceram. Soc., 62 (9-10), 528-529 (1979).
- [40] M-C. Bay, M. Wang, R. Grissa, M. V. F. Heinz, J. Sakamoto and C. Battaglia, "Sodium plating from Na-b"-alumina ceramics at room temperature, paving the for fast charging all solid state batteries, Adv. EnergyMater (2020) 10, 1908994139]
- [41] L. Viswanathan and A. V. Virkar, "Crack propagation rates in  $\beta$ "-alumina", J. Am. Ceram. Soc., 66 [3] (1983) 159-162.
- [42] Y. Lu, C.-Z. Zhao, H. Yuan, X.-B. Cheng, J.-Q. Huang, and Q. Zhang, "Critical Current Density in Solid-State Lithium Metal Batteries: Mechanism, Influences, and Strategies," Adv. Functional Mat. 31 (2021) 2009925.
- [43] A. V. Virkar, 'Failure of Ion-Conducting Materials by Internal Precipitation under Electrolytic Conditions', p.59-76, in 'Engineered Ceramics: Current Status and Future Prospects, Edited by T. Ohji and M. Singh, Wiley-American Ceramic Society (2016).
- [44] H-T. Lim and A. V. Virkar, 'A study of solid oxide fuel cell stack failure by inducing abnormal behavior in a single cell test', J. Power Sources, 185, 790-800 (2008).
- [45] R. D. Schmidt and J. Sakamoto, 'In-situ, non-destructive acoustic characterization of solid state electrolyte cells', J. Power Sources, 324 (2016) 126133.
- [46] S. Sarkar and V. Thangdurai, 'Critical current densities for high performance all solid-state Li-metal batteries: Fundamentals, Mechanisms, Interfaces, Materials and Applications,

- ACS Energy Letters, 2022 7 1492-1527.
- [47] E.C. Bingham, An investigation of the laws of plastic flow. US Bureau of Standards Bulletin, 13: 309-353, (1916).
- [48] A Sharafi, C. G. Haslam, R. D. Kerns, J. Wolfenstine and J. Sakamoto 'Controlling and correlating the effect of grain size with the mechanical and electrochemical properties of Li7La3Zr2O12 solid-state electrolyte', J. Materials Chem A, (2017) 521491-21504